Performance Enhancement of Solar Cooker Integrated with Photovoltaic Module and Evacuated Tubes Using ZnO/Acalypha Indica Leaf Extract: Response Surface Study Analysis

Arulraj Simon Prabu (s.shanmugam1982@gmail.com)
Sriram Engineering College https://orcid.org/0000-0002-7974-5675

Venkatesan Chithambaram
PERI Institute of Technology

Sengottaiyan Shanmugan
Koneru Lakshmaiah Education Foundation

Pasquale Cavaliere
University of Salento: Universita del Salento

Shiva Gorjian
Tarbiat Moallem University of Sabzevar: Hakim Sabzevari University

Abderrahmane Aissa
Université Mustapha Stambouli Mascara: Universite Mustapha Stambouli Mascara

Abed Mourad
Université Mustapha Stambouli Mascara: Universite Mustapha Stambouli Mascara

Pokkunuri Pardhasaradhi
Koneru Lakshmaiah Education Foundation

Rajamanickam Muthucumaraswamy
SVCE: Sri Venkateswara College of Engineering

Fadl Abdelmonem Elsayed Essa
Kafrelsheikh University

Ammar Hamed Elsheikh
Tanta University

Research Article

Keywords: Electrical backup, Evacuated tubes, Photovoltaic panel, thermal model, Solar cooker

Posted Date: April 28th, 2022

DOI: https://doi.org/10.21203/rs.3.rs-1512491/v1

Performance Enhancement of Solar Cooker Integrated with Photovoltaic Module and Evacuated Tubes Using ZnO/Acalypha Indica Leaf Extract: Response Surface Study Analysis

Arulraj Simon Prabu[1,2*], Venkatesan Chithambaram[3], Sengottaiyan Shanmugan[4*], Pasquale Cavaliere[5], Shiva Gorjian[6], Abderrahmane Aissa[7], Abed Mourad[7], Pokkunuri Pardhasaradhi[8], Rajamanickam Muthucumaraswamy[1], Fadl Abdelmonem Elsayed Essa[9], Ammar Hamed Elsheikh[10]

[1] Research Centre of Mathematics, Sri Venkateswara College of Engineering, 602 105, Sriperumbudur, India.

[2]Department of Electronics and Communication Engineering, Sriram Engineering College, Perumalpattu, Chennai, Tamil Nadu, India – 602024.

[3] Department of Physics, Peri Institute of Technology, Tambaram, Mannivakkam, Tamil Nadu 600048, India.

[4] Research Centre for Solar Energy, Department of Physics, Koneru Lakshmaiah Education Foundation, Green Fields, Guntur District, Vaddeswaram, Andhra Pradesh 522502, India.

[5] Department of Innovation Engineering, University of Salento, 73100, Lecce, Italy.

[6] Biosystems Engineering Department, Faculty of Agriculture; and Renewable Energy Department, Faculty of Interdisciplinary Science & Technology, Tarbiat Modares University (TMU), Tehran, Iran.

[7] Laboratoire de Physique Quantique de La Matière Et Modélisation Mathématique (LPQ3M), Université Mustapha Stambouli de Mascara, Mascara, Algeria

[8] Dept of ECE, Koneru Lakshmaiah Education Foundation, Green Fields, Guntur District, Vaddeswaram, Andhra Pradesh 522502, India.

[9] Mechanical Engineering Department, Faculty of Engineering, Kafrelsheikh University, Kafrelsheikh 33516, Egypt.

[10] Department of Production Engineering and Mechanical Design, Faculty of Engineering, Tanta University, Tanta 31527, Egypt.

Emails IDs: (Simon) simonprabu07@gmail.com, (Chithambaram) chithambaramv@gmail.com, (Shanmugan) s.shanmugam1982@gmail.com, (Cavaliere) pasquale.cavaliere@unisalento.it, (Shiva) Gorjian@modares.ac.ir, (Aissa) a.aissa@univ-mascara.dz, (Abed) mourad.abed@univ-mascara.dz, (Pardhasaradhi) pspokkunuri@gmail.com, (Muthucumaraswamy) msamy@svce.ac.in, **(Essa)** fadlessa@eng.kfs.edu.eg, (Ammar) ammar_elsheikh@f-eng.tanta.edu.eg**.**

Corresponding authors, *E-mail addresses:

(Simon) simonprabu07@gmail.com,

Abstract

In this study, the effect of employing ZnO/Acalypha Indica leaf extract (ZAE) on the energy absorption of a coated portable solar cooker have been examined using an experimental setup. A prototypical model has been developed to corroborate in associating an investigative outcome per constituents of the experiments. The studied heat transfer process in ZAE is stable for harsh conditions. The design analysis and an estimation of the system performance were done given various parameters including the pressure of the vacuum envelope, bar plate coating digestion, emissivity, and solar rays. The fabricated solar was tested with and without ZAE to investigate the impact of this coating material on the solar cooker's thermal performance. To observe the performance of the new design, two figures of merit (F_1 and F_2) have been introduced. The factual food cooking assessments were for a family of four people, which operated in ZAE coating (0.8, 1.0, 1.2 μm) of the solar cooker. The values of F_1 and F_2 for the proposed cooker were obtained as 0.1520 and 0.4235, respectively, which is intact with the BIS values. The results revealed that employing ZAE instead of a thermal NHC - PV solar cooker reduced the time required to boil 2 L of water for about 2,820 seconds. The overall thermal energy productivity of the solar cooker with electrical backup was obtained as 42.65%, indicating that the ZAE coating can improve the thermal efficiency by 10.35%.

Keywords: Electrical backupz Evacuated tubes; Photovoltaic panel; thermal model; Solar cooker

1 Introduction

A solar cooking process is a method in which solar radiation is utilized to naturally cook substances. Research worldwide have found out that solar cookers have sustainability for cooking in rural and urban areas with reduced energy consumption. A solar cooker using sun radiation as a heat source, can be utilized on hot sunny days, but on rainy and winter days it is useless. It has been found that a solar cooker with an electrical backup will overcome these inconveniences. An electric backup integrated with a solar cooker has shown better performance compared to the cooker supported with thermal energy alone. Moreover, selectively coated absorbers using nanoparticles play an important role in enhancing the performance of solar cookers. Several studies have assessed the effect of selective absorber coating using nanoparticles. Kaiyen et al. (2009) used a light funnel to congregate solar energy to achieve temperature suitable for industrial and

domestic usage. It was identified that a temperature of 250 °C is achieved with a lighting area of 1.5 m^2. Prasanna and Umanand (2011) experimented by transferring solar energy to the kitchen using fluid circulation to stimulate a cooker using the concept of maximum power point tracking (MPPT) for a thermal collector. Javadi et al. (2013) also reviewed the effect of using nanofluids on the performance of solar collectors. In their review, care was taken to highlight the impact of two-phase analysis of the nanofluid with more than one nanoparticle in the heat transfer fluid. Hussein et al. (2017) reviewed theoretical, numerical, and experimental studies of a heat pipe solar collector incorporating a nanofluid. They reported that various research works have proved the significance of nanofluid in improving the thermal performance and efficiency of solar collectors. Palanikumar et al. (2019) fabricated a solar box-type cooker (SBC) including a phase change material (PCM) and nanoparticles coating in the design and evaluated its performance with thermal imaging of the structure. Then, they used a fuzzy logic algorithm to develop a model to predict the thermal performance of the solar cooker. The results of the study revealed that when eggs are boiled, the thermal performance of the solar cooker can reach 52.17% and 75.47%, utilizing PCM and nanoparticles, respectively.

Furthermore, Bhavani et al. (2019) designed an SBC and coated it with black paint and nanoparticles. Then the design was evaluated using fuzzy logic rules. From the results, it was found that using nanoparticles in the coating enhances the thermal efficiency of the solar cooker by 7.10%. The fuzzy logic rules have also been utilized in other studies to model solar cookers. Such as Palanikumar et al. (2021) and Venugopal et al. (2012). Thamizharasu et al. (2022) developed a stepped SBC (SSBC) coated with silicon dioxide (SiO_2) and titanium dioxide (TiO_2) nanoparticles and analyzed them at different volume fraction ratios of nanoparticles between 5% to 25%. The findings indicated that the overall thermal efficiency of the solar cooker can be improved by 31.42% when using the SiO_2/TiO_2 nanolayers at 15% volume fractions of nanoparticles. In another study by Thamizharasu et al. (2021) the solar cooker was analyzed using an adaptive control method which was modeled using the online sequential extreme learning machine (OSELM), and the heat analysis of the system was made in the Binary Search Tree data structure. From the results, the efficiency of the solar cooker was obtained as 49.21% for a 15% volume fraction of SiO_2/TiO_2. Palanikumar et al. (2021) performed a comparative study on a fabricated SBC, this include an SBC with PCM, and an SBC with PCM and a nanocomposite (NPCM). After analysing the fuzzy logic and Cramer's rules, image processing techniques were applied. The results indicated that coating

the bar plate absorber with nanoparticles and integrating a PCM increases the internal temperature of the SBC up to 164.12 ℃, and enhance the overall thermal efficiency by 11% compared to the other tested configuration (2019). Palanikumar et al. (2020) studied an SBC coated with a nanocomposite film containing tantalum pentoxide (Ta_2O_5) doped with stannic oxide/Silver. The results indicated that the spectrally selective characteristic is improved and the bar plate temperature reaches 203.33 °C.

Shinde et al. (2016) utilized preheated water to increase the thermal efficiency of a large-scale cooker with three levels of screw speed, solid flow rate, and liquid flow rate. The results indicated that the required time for batch cooking is equivalent to the minimum residence time. Cerium oxide (CeO_2) nanoparticles of 25 nm were prepared and combined with heat transfer fluid, including water in different concentrations by Sharafeldin and Gróf (2018). The obtained nanofluid was used in solar evacuated tube collectors (ETCs) to improve thermal performance. It was found that the thermo-optical characteristics were increased by 34%. Khallaf et al. (2020) also fabricated a Quonset solar cooker with dome-shaped polymeric glaze incorporated with internal reflectors and performed experimental and theoretical analysis. The study revealed that cooking fluid glycerine gives efficiency ranging from 9% to 92% during cooking hours. The solar cooker's energy and exergy efficiencies with multiwalled carbon nanotube-oil nanofluid were investigated with varying volumetric flow rates by Hosseinzadeh et al. (2021). It was found that nanofluid-based solar cooker gives improved efficiency of 37.30% and 65.87% for 0.2% and 0.5% wt concentration in oil, respectively. Mallikarjuna et al. (2021) reviewed the effect of nanofluids to enhance the heat transfer rate in solar energy harvest. The results of different research works conducted by various researchers have been presented in more detail in their study.

Bo Liu et al. (2021) carried out studies using zinc oxide (ZnO), SiO_2, copper oxide (CuO), aluminum oxide (Al_2O_3), and carbon derivative nanomaterials on copper, silicon, SiO_2, aluminum, and stainless-steel substrates and found the enhancement of thermal performance of the absorbers due to selective absorber coatings. Alshukri et al. (2018) used micro ZnO and nano CuO nanoparticles with paraffin wax in a solar heat-pipe ETC. The results indicated that the efficiency increases in the range of 33.8% to 45.7%. A comprehensive review regarding the various kinds of nanofluids in ETCs was conducted by Vijayakumar et al. (2021), and conclusions were highlighted with the performance enhancement of the ETCs. Vengadesan and Senthil (2021) fabricated finned cooking vessels with a variable length of 25, 35, and 45 mm and evaluated them. It was found out

that the fin length of 45 mm gives higher thermal efficiency of 50.03% with a heat transfer coefficient of 58.54 W/m^2°C. Hosseinzadeh et al. (2021) used different nanofluids in a solar collector and cooking unit and performed energy and exergy analyses. The study indicated that employing silicon carbide (SiC) nanofluid in the system provides good performance in which 2 L of water boiled in 17 min. Shehayeb et al. (2021) employed cathodic electrophoretic deposition to enhance the optical properties of the CuO tandem solar absorber. It was observed that the fabricated tandem absorber provides enhanced efficiency.

Based on the reviewed literature presented supra, it is clear that a number of studies have been conducted to assess the impact of nanoparticles on the performance of various solar cookers. This study therefore uses ZnO/Acalypha Indica leaf extract (ZAE) and black mat paint on the sides and bottom of a cooking vessel to enhance its performance. A mathematical model has been proposed, and the validation of the analytically obtained results is obtained through experimental observations. Moreover, two figures of merit F_1 and F_2 were proposed to evaluate the solar cooker performance with and without using ZAE with black mat paint.

The rest of the study is presented in the following order, the materials and method used for the study are presented in section 2, section 3 presents the results and discussion, whiles the conclusions made on the study is presented in section 4.

2 Materials and methodology

2.1 Preparation of Acalypha Indica leaf extract

Fresh Acalypha Indica leaves were collected in March 2021 in Mellampude, Vijayawada - AP, India. The surface of the leaves was cleaned with running tap water to remove the dust and other contaminated organic compounds, followed by distilled water and dried at room temperature for 15 days (total count of 1,000 leaves). The dried leaves were collected and then about 30 g of the collected leaves were taken and mixed with 300 mL of distilled water. The prepared sample was then heated and stirred at 50 °C for 3 h. The solution was boiled at 70 °C for 20 min. The color of the solution changed to green which indicates the formation of a leaf extract. The obtained solution was filtered with Whatman No. 1 sieve paper to obtain a clear extract. Then Acalypha Indica extracts were filtered two times and pure samples were collected and maintained at 5 °C. The extract samples were prepared to be directly utilized in synthesis experimentations as shown in **Fig. 1(a)**.

158

159 *2.2 Preparation of ZnO using Acalypha Indica leaf extract (ZAE)*

160 The experimental materials were prepared and all chemical materials were purchased from the
161 company AR Scientific, Basaveshwara Layout, Bengaluru, and Karnataka 560094. Zinc acetate
162 dihydrate (99.7%) and ethanol (99.5%) chemicals as standard cleaning agents in experimental
163 works were obtained from the Research Centre for Solar Energy at Vijayawada civic KLEF India.
164 A 2 g nickel nitrate (Ni $(NO_3)_2$) was added to 200 mL of distilled water and allowed to stir for 20
165 min. The solution was added in drops to the leaf extract under constant stirring for 2 h using a
166 magnetic stirrer (Ghamsari et al, (2019); Alamdari et al, (2019); Alamdari et al, (2017); Alamdari
167 et al, (2015);Vafaee et al, (2011) as shown in **Fig. 1(b)**. The solution was then dried on a hot plate
168 to obtain a powder form. Finally, the nickel oxide (NiO) sample was prepared. The powder was
169 then placed in a muffle furnace at a temperature of 500 °C for 3 h in ZnO/Acalypha Indica stem
170 extract, as shown in **Fig. 1(c)**. The obtained sample can be used in further studies. **Fig. 1(d)** shows
171 this process and the establishment of chemical bonds structure and extracted with particles of ZnO
172 using Acalypha Indica Leafs.

173 *2.3 2.3 Characterizing of ZnO/ Acalypha Indica extract*

174 *2.3.1 X-ray diffraction*

175 **Fig. 2(a)** shows the X-ray diffraction (XRD) pattern of NiO nanoparticles (NiO-Z)
176 prepared using Acalypha Indica leaf and stem extract (AE). In the XRD analysis, the x-axis
177 represents 2θ, and the y-axis indicate the intensity of the peak. The presence of 2θ for ZAE
178 corresponds to (1 1 1), (2 0 0), (2 2 0), and (3 1 1) & (1 1 1), (2 0 0), (2 2 0), (3 1 1), and (2 2 2)
179 orientation confirms the presence of NiO particles in a cubic structure. The grain size (D) of the
180 nanoparticles was calculated using the Debye-Scherrer formula using the reflection form of the
181 XRD pattern. Debye-Scherrer formula for grain size is presented in Eq. (1):

182 $$D = 0.9\lambda / \beta \cos\theta \quad (1)$$

183 where D is the grain size, λ is the wavelength of copper (1.54Å), β is the full width half maximum
184 after correcting the instrument peak broadening (β expressed in radians), and θ is the Bragg's
185 angle. In this XRD analysis, the grain size of NiO using ZAE was calculated as 20.61938×10^{-9} m
186 and 22.3126×10^{-9} m, respectively. The Lattice Parameter (a) was calculated using Eq. (2).:

187 $$a = d\sqrt{(h^2+k^2+l^2)} \quad (2)$$

where d is the interplanar spacing value; h, k, and l are Miller indices. The Lattice Parameter of ZAE has been calculated as 4.20825Å and 4.17629Å. The Cell Volume (a^3) is calculated from the value of Lattice Parameter (a). Therefore, the value of the Cell Volume for ZAE is calculated as 52.544 ($Å^3$) and 72.84033 ($Å^3$).

2.3.2 Fourier Transform Infrared Spectroscopy (FTIR) analysis

Fourier Transform Infrared Spectroscopy (FTIR) is a technique use to obtain an infrared spectrum of absorption or emission of a solid, liquid, or gas. An FTIR spectrometer simultaneously collects high spectral resolution data over a wide spectral range. The Fourier Transform Infrared Spectroscopy (FTIR) investigation was carried out using PERKIN ELMER (Spectrum RXI) spectrometer in 400 cm^{-1} to 4000 cm^{-1}. The functional groups were identified using the peaks assignments. **Fig. 2(b)** shows the FTIR spectrum of nickel oxide nanoparticles using ZAE in **Table 1.**

2.3.3 Analysis of UV Spectrum

This study mixed the Nickel nitrate source with the plant extract of the Acalypha Indica leaf and stem extract. The color of the AE changes from brown to dark green, the color of NiO (Z) also changes from yellow to light green. These color changes are due to the excitation of surface Plasmon vibrations. The UV-visible spectrum x-axis indicate wavelength whiles the y-axis indicate absorption. AE represents nickel oxide (Ni_2O_3) nanoparticles using Acalypha Indica Leaf extract in the UV spectrum, and Z represents ZAE. In this spectrum, the range of Ni_2O_3 nanoparticles using leaf and stem extract was reported in the range of 293 nm and 291.3 nm as shown in **Fig. 2(c).** The corresponding absorptions are also identified. It indicates the possibility of the formation of Nickel Oxide nanoparticles, and in this spectrum, comparing the two ranges, we observed that the AE is better than ZAE.

2.3.4 SEM and EDAX analyses

The surface morphology of the resulting powder was examined using a scanning electron microscope. **Fig. 2(d)** indicates that AE and ZAE were observed within the range of × 10,000 and × 10,000. The image shows that the morphology of Ni_2O_3 nanoparticles is a spherical shape for AE and in coral reef structure for ZAE without any agglomeration in nano size. From the EDAX (Energy Dispersive X-Ray Analysis) spectrum image, elements in the Acalypha Indica leaf and

stem extract are evident. The EDAX spectrum of nickel oxide nanoparticles were used, whiles that of ZAE shows only the peak of nickel (Ni) and Oxygen (O_2) elements. ZAE shows only the peak of nickel (Ni), and oxygen (O) elements, which confirms that the prepared nickel nanoparticles are essentially free from impurities and are at the limit of EDAX. Identification lines for the significant emission energies for Ni, O_2 and thus correspond with the peak in the spectrum; thus, nickel has been identified correctly as shown in **Fig. 2(e).** The AE atomic weight percent values of Ni, O have been absorbed, 38.98, 57.79. The ZAE atomic weight percent values of Ni, O that have been observed are 41.98, 55.17.

2.4 Design of the solar cooker

The compatible solar cooker has three components with evacuated tubes with a high vacuum ($P < 5 \times 10^{-3}$ m bar) enclosed in a rectangular wooden box with parabolic trough reflectors (PTRs)

- Solar photovoltaic (PV) panel (2 x 100W);
- 12 V 75AH Battery;
- Stove with two vessels for cooking.

A compatible solar cooker with a PV panel and evacuated tubes (Solar Chulha) was designed and fabricated. Evacuated tubes have a high vacuum ($P<5 \times 10^{-3}$ Pa) used in the proposed cooker, and it is used to produce hot water of about 75°C for cooking. PTRs were designed, and the evacuated tubes were fixed on the focal line of the trough to receive maximum solar radiation. The copper tubes carrying the heat transfer fluid (water) were made to run through the evacuated tubes to extract the thermal energy received by the tube. The temperature of the heat transfer fluid at the outlet was high. A PV panel with a power output of 200 W was used to charge a 12V 75 AH battery. The electricity drawn from the battery was used to heat the heating filament (Nichrome) covering the cooking vessel. Hot water from the evacuated tubes was further heated up to the boiling point, and the food was cooked quickly. The DC power produced by the panel was stored in the battery during the daytime to be used at night. **Fig. 3(a)** and **Fig. 3(b)** show the solar cooker's photograph and its different components. Among the two cooking vessels, one vessel was coated with ZAE and mat black paint on the sides and base of the cooking vessel, and the other vessel with only black mat paint.

2.5 Experiment performance

Two cooking vessels are used with and without coated ZAE sides in which the vessel's bottom, was subjected to stagnation temperature test without any load in the vessel. The cooking vessels by the bottom (base) and the absorber were allowed to absorb thermal energy via the sides and bottom of the vessel. Thermal energy was produced by the Nichrome heating coil and conducted through the sides and bottom of the vessel, coated with black mat paint with and without ZAE. The experiments were carried out to find the figure of Merit F_1, which is a function of stagnation temperature. F_1 is calculated from the Standard formula presented in Eq. (3) (Alamdari et al (2019)):

$$\boldsymbol{F_1 = \frac{T_{bs} - T_a}{H}} \tag{3}$$

Table 2 represent the variation of temperature at the base of the two cooking vessels with and without ZAE. The observed first figure of merit (F_1) for the cooking vessels with and without ZAE was 0.1520 and 0.1143, respectively. Due to the enhanced heat transfer from Nichrome heating coil to the sides and base of the cooking vessel with a coating of ZAE along with black mat paint, and also, the thermal stability of ZAE led to a good thermal conduction of the thermal energy transferred to the cooking vessel, as shown in **Fig. 4(a).**

From the graph, the temperature of the cooker's base with ZAE with black mat paint is noticeable throughout the path towards the stagnation temperature of 133°C compared to the vessels without ZAE. According to the Bureau of Indian Standard, the F1 value of 0.12 km^2/W is significant, and in the present cooker, the value is 0.1520 km^2/W. A Figure of Merit (F_2) was found by experimenting with the proposed solar cooker with load (sensible heat material), i.e., 1 kg of water in the cooking vessels with and without a coating of ZAE on the sides of the bottom of the vessel.

2.5.1 Second Figure of Merit (F_2)

The cooker performs based on the sensible heating of a load inside. The proposed cooker was filled with a sensible load of 1 kg of water in the two cooking vessels with and without a coating of ZAE and black mat paint on the sides and bottom of the vessel. F_2 can be calculated using the expression presented in Eq. (4):

$$F_2 = \frac{F_1 (MC)_w}{A(t_2 - t_1)} ln \left[\frac{1 - \left(1/F_1\right)}{1 - \left(1/F_1\right)} \frac{((T_{w1} - T_a)/H}{((T_{w2} - T_a)/H} \right] \tag{4}$$

Measurements were done to find the second figure of merit, and they are:

(i) Cooking fluid temperature at a regular time interval until the fluid temperature reaches a maximum of 95°C.

(ii) Duration of time between the initial and final cooking fluid temperature

(iii) The intensity of solar radiation and ambient temperature were measured using a solar radiation monitor and digital thermometer.

Table 3 characterizes the data collected from the measurements made during the testing for the Second Figure of the Merit of the solar cooker.

2.5.2 Interval Cooking Power (P)

It is also called average cooking power (P) which means the helpful energy available during the cooking period. It is defined as the ratio of increase in temperature of the cooking fluid for each interval of time multiplied by the mass and specific heat of the cooking fluid to the time interval specified, and the expression given as indicated in Eq. (5).

$$P = \frac{(MC)_w(T_2 - T_1)}{600} \quad (5)$$

2.5.3 Standardized cooking power (P_s)

Standard solar insolation of 750 W/m^2 for each interval has been used, and utilizing Interval cooking power (P), the standardized Cooking Power (P_s) can be evaluated using Eq. (6).

$$P_s = \frac{P \times 750}{H} \quad (6)$$

Table 4 represents the variation of interval cooking power and standardized cooking power during the testing load for the second figure of merit.

From **Fig. 4(b),** it is understood that the standardized cooking power is a function of Interval Cooking Power (P) and is inversely proportional to the intensity of solar radiation during the interval of time. Interval cooking power is the functional difference in initial and final temperature during the time interval with a standard intensity of solar radiation of 600 W/m^2. Moreover, the standardized cooking power has a conjoint trend concerning the interval cooking power at each time interval with power less than that of the interval cooking power.

2.6 Thermal Modeling

Since the cooker is incorporated with the evacuated tube, it can obtain preheated cooking fluid from the outlet of the evacuated tubes. The temperature of the cooking fluid at the outlet is considered the initial temperature of the cooking fluid in the cooking vessel. The base and sides of the cooking vessel are surrounded by the Nichrome heating coil, which receives the current from the solar panels of 200 W each. The base and sides of the cooking vessel are coated with ZAE to enhance the heat conduction of the vessel to deliver the auxiliary heat to the preheated cooking fluid. Since the nanoparticles play a vital role in transferring the heat from the nichrome heating coil to the cooking fluid, it will reduce the cooking time for the foodstuff reasonably. Here, energy balance equations have been written for the cooking fluid, base and sides of the cooking vessel and solved for the analytical solution.

The base of the cooking vessel:

$$P_e A_b \times t + T_{out} A_b SM = h_{bs} A_b (T_b - T_a) + h_{cbcf} (T_b - T_w) \quad (7)$$

Sides of the cooking vessel:

$$P_e A_s \times t + T_{out} A_s SM = h_{bs} A_s (T_s - T_a) + h_{cscf} (T_s - T_w) \quad (8)$$

The outlet water from the evacuated tube into the cooking vessel absorbs energy given by the Nichrome heating coil through the base and sides of the cooking vessel. Since the base and sides of the cooking vessel are coated with ZAE, heat energy is convected to the preheated cooking fluid. Due to an effective heat transfer from the Nichrome heating coil to the cooking fluid through the ZAE coated base and sides of the cooking vessel, the cooking fluid absorbs much more energy. The temperature of the fluid increases rapidly. As a result, the time for cooking the food in the proposed cooker is reduced.

The lid of the cooking vessel:

$$h_{cfl} (T_w - T_l) = h_{la} (T_l - T_a) \quad (9)$$

Cooking fluid

$$M_w C_w \, {dT_w}/{dt} + h_{cbcf} (T_b - T_w) + h_{cscf} (T_s - T_w) = h_{cfl} (T_w - T_l) \quad (10)$$

Eqs. (7), (8), and (9) have been solved for T_b, T_s, and T_l, and substituted in Eq. (10). Rearranging Eq. (10) and can be written as

$$\frac{dT_w}{dt} + aT_w = f(t) \quad (11)$$

where a and $f(t)$ are constants, this can be obtained from the equations on temperature components of the evacuated tube collector, Nichrome heating coil, and cooking vessel. At $t=0$, $T_w = T_{w0}$, and due to the initial condition, we can write the solution of the equation as

$$T_w = \frac{f(t)}{a}(1 - e^{-\propto t}) + T_{w0}e^{-\propto t} \quad (12)$$

where α is a constant and depends on the different heat transfer coefficients of the cooker. The photovoltaic with evacuated tubes which connects the nichrome heating coil utilized in the solar cooker's input and output has been calculated and the overall energy efficiency (η_{ZAE}) can be written as presented in Eq. (13)

$$\eta_{ZAE} = \frac{E_{\mathrm{NHC,out,ave}} - \frac{E_p}{\eta_{pv}}}{A_{sc}\int_{t_1}^{t_2} H\, dt} \quad (13)$$

3 Results and Discussion

This research work is focused on the effect of the presence of ZAE coating and its thickness on the thermal performance of a solar cooker.

3.1 Effect of ZAE coating thickness

An experiment was carried out with the proposed cooker during summer and winter days under local climatic conditions of Vijayawada, Andhra Pradesh, India. The analytical solutions of the energy balance equations for the temperature elements of the cooker were used to evaluate the temperature of the base, sides, and lid of the cooking vessel, followed by the temperature of the cooking fluid. The climatic parameters during the experiment were recorded using the solar radiation monitor and digital thermometer. Calibrated copper-constantan thermocouples were used to measure the temperature of the cooker.

The impact of varying the thickness of the ZAE coating on the performance of the solar cooker and the overall thermal efficiency was investigated, where tested thicknesses are 0.8-micron, 1.0-micron, and 1.2-micron. It was found that the coating thickness with the best absorption solar energy and ambient temperature on the design is 1 micron of the ZAE material. The performance of the solar cooker with a 1.0-micron coating was measured and analyzed from June 2020 to June 2021. The solar cooker with a one-micron thickness coating of ZAE was absorbed in more solar radiation and ambient temperature during experimental average values compared to others with different thickness levels. KLEF climate conditions utilization of the solar cooker has improved

performance in more absorption by solar radiation around 25W/m^2 and ambient temperature is 4°C, individually.

3.2 Effect of the presence of ZAE coating

An output thermal influence analysis of a design was utilized. We are focused on the best-performing thickness which was chosen as one micron as demonstrated in **Fig. 5(a).** Cooking vessels with and without the ZAE coating (one micron) were filled with 1 kg of water. The experimental work was performed until the temperature of the sides and base of the cooking vessel reached its stagnation temperature. **Fig. 5(b)** represents the variation of the temperature of the cooking vessel's side, base, and lid. The base and sides of the vessels with and without ZAE were experimented for their activity to find the impact of ZAE coating. From the figure, it is observed that the temperature of the vessel with a coating of ZAE has dominated temperature at each measurement in regular intervals and proved that the ZAE enhanced the conduction of thermal energy from the Nichrome heating coil to the base and sides of the cooking vessel. Moreover, ZAE has a significant capacity to transfer heat energy to the cooking fluid through the base and sides of the cooking vessel. Furthermore, validation of the model was performed for the temperature of the base, sides, and lid of the cooking vessel with the analytical solutions obtained by solving the energy balance equations of the temperature elements of the cooker.

Fig. 5(c) shows the variation of the theoretical and experimental values of the temperature of the base, side, and lid of the cooking vessel with a coating of ZAE. It was observed that both the theoretical and experimental values have a conjoined trend with maximum coincidence. Standard deviation between the experimental and theoretical values ensures the validation of the model. For the temperature of the base, side, and lid of the vessel, the standard deviation values between the experimental observation and theoretical values were 0.025, 0.109, and 0.0416, respectively. The mathematical model calculated precise values for temperature elements of the cooker which agree with the experimental observations.

3.3 Experimental and theoretical cooking values analysis

The cooking fluid's temperature was used to find the theoretical values and compared with the experimental observations by finding the standard deviation between the experimental and theoretical values. **Fig. 5(d)** represents the variation of the experimental and theoretical values of

cooking fluid temperature concerning that of time with a load of 1 kg of cooking fluid in the cooker.

Preheated water from the ETC with a temperature of 76°C entered the cooking vessel. The temperature of the preheated water was taken as the initial temperature of the cooking fluid in the cooking vessel with a coating of ZAE on the sides and the base. The preheated water reached a maximum temperature of 96°C within 15 min with the auxiliary heat obtained from the Nichrome heating coil through the base and sides of the cooking vessel. The energy balance equation for the cooking fluid was considered to evaluate the temperature of the cooking fluid during the cooking time. The theoretical values for the temperature of the cooking fluid were compared with the experimental observation by finding the standard deviation between them. From the graph, it is clear that both the experimental and theoretical values have conjoined trends throughout the working period. It was found that the average standard deviation between the experimental and theoretical values is 0.16122, which was expected.

3.4 Cooking performance

The new design was analyzed for different thicknesses of ZAE coating for a given water temperature inside the solar cooker as shown in **Fig. 6(a).** The solar cooker's values were recorded during the heating of water (2 L), which was performed with coating with various ZAE thicknesses, the time required for cooking decreased from 102 min to 58 min, 47 min, and 54 min. That is, 58 minutes (0.8 μm), 47 minutes (1.0 μm), and 54 minutes (1.2 μm) and without ZAE coated test the obtained values are 102 min by the system. The analysis of the solar cooker with ZAE coated in 1.0-micron show that the average time to boil a 2 L water increased by 24.32 min (32.26%) from June 2020 to June 2021.

The absorbed energy by the 2 L of water can reduce the cooking time and obtain over a time intermission of 15 min. The performance of the solar cooker is established with output period intermissions, and the cooking ends at a constant temperature. As indicated earlier, ZAE coating in the solar cooker was found to enhance the cooking performance by absorbing more thermal energy from the bar plate. The PV power and nichrome heating coil were also connected with the solar cooker to increase the internal heat transfer modes, thereby increasing the thermal heat flow rate of the system. The experiments proved that the mathematical modeling for the proposed

cooker could be utilized to optimize design parameters for large-scale installation to serve large communities. Further, the model can be used to evaluate the proposed cooker in any other location with a similar climatic condition to study its performance.

The proposed cooker with cooking vessels with and without the ZAE coating (one micron) was evaluated to cook various kinds of food stuffs. The time taken for cooking with both vessels is tabulated in **Table 5**. The cooking time for various foodstuff in **Table 5** demonstrate that the cooking period for the vessel with ZAE coating reduced compared to that of the vessel without coating. Additionally, a cooker size of 24 × 7 can be used by a family of 4 members short of intermission. During the daytime, one can use the cooker by incorporating the thermal energy received from the evacuated tubes supported by electrical backup provided through the Nichrome heating coil. In the nighttime, the battery can be discharged to supply current through the Nichrome heating coil to fulfill the required energy for cooking in the vessel.

3.5 Design performance of ZAE mass fraction

The solar cooker with impact of using ZAE coated with 0.8-micron, 1.0 micron, and 1.2-microns on the overall performance of the solar cooker is assessed from the perspective of thermal energy. Also, the impact of the presence and absence of the ZAE coating (one micron) on the solar cooker's performance was evaluated and discussed in Section 3.1. It established that the solar cooker has been analyzed with coated samples in different micron levels including 0.8, 1.0, and 1.2, with enhanced thermal energy productivities compared to the other cases. The solar cooker is achieved in one micron used in the investigation. Average solar radiation during the model was 789.43 W/m^2, 791.27 W/m^2, and 785.11 W/m^2 for the test with the ZAE coated solar cooker with 0.8-micron, 1.0 micron, and 1.2 microns, respectively. The ambient temperature values were also 34.77 °C, 35.28 °C, and 34.73 °C, respectively, indicating that the achieved model is somewhat comparable with the climatic environmental conditions.

3.6 Efficiency analysis

One of the solar cooker vessels was coated with ZAE materials using different micron levels and the impact of this variable on the heat transfer and productivity of the solar cooker is shown in **Fig. 6(b).** The coated section with ZAE increased the thermal energy absorption which in turn enhanced its heat transfer characteristics. This consequently increased the energy efficiency of the system. The average design energy efficiency is found to be around 39.11%, 48.31%, and 41.24%, for heat

transfer with an efficient ZAE materials coating of 0.8-micron, 1.0 micron, and 1.2-micron thickness, respectively. The solar cooker performed with characteristics performance on ZAE as followed in **Table 6** as comparative studies.

4 Conclusion

An overall performance of a solar cooker using ZAE coating was investigated from a thermal energy performance point of view. Also, the output of a cooker using PV and evacuated tubes with cooking pots with and without ZAE coating were estimated. Investigated parameters in this research include ZAE coatings with different thicknesses of 0.8 micron, 1.0microns, and 1.2 micron, which were used in the ZAE mass fraction of the system. The following conclusions are drawn from the current study:

(i) The ZAE coating on the sides and the base of the cooking vessel were evaluated in terms of F_1 (0.1520) and F_2 (0.4230) which are below the BIS (Bureau of Indian Standards) values of Indian Standards.

(ii) The mathematical model was validated with a negligible difference in the cooker's experimental and theoretical temperature which was proved by finding the standard deviation between the theoretical and experimental observations.

(iii) For the temperature of the base, sides, lid, and cooking fluid, the standard deviation value between the experimental observation and theoretical values were 0.025, 0.109, 0.0416, and 0.16122.

(iv) The cooking time for various foodstuff in the cooking vessel with ZAE coating reduced significantly to save time.

(v) The thermal efficiency of the cooker was found to be 42.65% by incorporating the input energy with extra energy supplied through electrical backup. When ZAE coating was used, the efficiency was enhanced by 10.35% compared to the cooking vessel without the coating.

(vi) The newly designed solar cooker with ZAE coating was used on a 24 x 7 basis as necessary to cook for a family of 4 which proves its reliability.

Consequently, the utilization of ZAE as a coating material for the solar cooker was found to be a suitable technique to improve the thermal performance of a solar cooker. In addition, phase change material (PCM)-based energy storage materials when integrated into a solar cooker can offer the

possibility of cooking after sunset. Therefore, the upcoming study will be to investigate the consequences of simultaneous use of ZAE and PCM to improve the energy productivity of solar cookers.

Nomenclature

A	-	Area of the base and side of the cooking vessel (m^2)
A_{sc}	-	Solar cooker area (m^2)
C	-	Specific heat capacity of water (J/kgK)
$E_{\mathrm{NHC,out,ave}}$	–	average energy output in NHC (%)
E_p	-	Energy pump
$F_{1\&2}$	-	First and second Figure of Merit
H	-	Intensity of Solar Radiation (W/m^2)
$H\ dt$	-	Hourly variation of solar radiations (W/m^2)
h_{cbcf}	-	Convective heat transfer coefficient from base of the cooking vessel to cooking fluid (W/mK)
h_{cscf}	-	Convective heat transfer coefficient from side of the cooking vessel to cooking fluid (W/mK)
h_{cfl}	-	Convective heat transfer coefficient from cooking fluid to the lid of the cooking vessel (W/mK)
h_{la}	-	Convective heat transfer coefficient from the lid of the cooking vessel to the ambient (W/mK)
M	-	Mass of water (kg)
P	-	Interval cooking power (W)
P_s	-	Standardized Cooking power (W)
T_a	-	Ambient Temperature (°C)
t_1	-	Initial time
t_2	-	Final time
T_{w1}	-	Initial water temperature (K)
T_{w2}	-	Final Water Temperature (K)
T_1	-	Initial water temperature during the evaluation of Interval Cooking Power (°C)

T_2	-	Final water temperature during the evaluation of Interval Cooking Power (°C)
M_w	-	Mass of cooking fluid (kg)
C_w	-	Specific heat capacity of cooking fluid (J/kgK)
T_w	-	Temperature of cooking fluid (°C)
T_b	-	Temperaure of the base of the cooking vessel (°C)
T_s	-	Temperature of the sides of the cooking vessel (°C)
T_l	-	Temperature of the lid of the cooking vessel (°C)
T_a	-	Temperature of the ambient (°C)
T_{ps}	-	Stagnation temperature of the base of the cooking vessel without load (°C)
η_{pv}	-	Overall output of PV

Funding Statement

The authors would like to thank the Department of Science and Technology (DST, Delhi), Government of India for the award of the DST-FIRST Level-1(SR/FST/PS-1/2018/35) scheme to the Department of Physics. Appreciations are grateful to the KLEF offering infrastructure, facilities, basic found (Perform basic instruments) and support to the current investigation.

Conflict of Interest

There is no conflict of interest among the authors.

Author Contributions

A. Simon Prabu

Synthesis and characterization of SiO_2 NPs with herbal extracts

Dr. V. Chithambaram

Data validation, reviewing and editing the paper

Dr.S. Shanmugan

Analysis of results, writing the manuscript, reviewing and editing the paper

Dr. Pasquale Cavaliere and Dr. Shiva Gorjian

Data validation, Editing of the manuscript

Dr. Abderrahmane Aissa and Abed Mourad

Analysis of results

Dr. P. Pardhasaradhi and Dr. R. Muthucumaraswamy

Analysis of results, writing the manuscript,

Dr. F. A. Essa and Dr. Ammar Hamed Elsheikh

Analysis of results, Data validation,

Availability of Data and Material

The synthesized materials with herbal extracts and data of results of characterization are available.

Compliance with ethical standard

The research work is ethically complied.

Consent to participate

All the authors give their consent to having participated in the current work.

Consent for publication

All the authors give their consent for publication of this work.

References

[1] Kaiyan H, Hongfei Z, Tao T, Xiaodi X (2009) Experimental investigation of high temperature congregating energy solar stove with sun light funnel. Energy Convers Manag 50:3051–5. https://doi.org/10.1016/j.enconman.2009.08.009

[2] Prasanna UR, Umanand L (2011) Optimization and design of energy transport system for solar cooking application. Appl Energy 88:242–51. https://doi.org/10.1016/j.apenergy.2010.07.020

[3] Javadi FS, Saidur R, Kamalisarvestani M (2013) Investigating performance improvement of solar collectors by using nanofluids. Renew Sustain Energy Revm28:232–45. https://doi.org/10.1016/j.rser.2013.06.053

[4] Hussein AK, Li D, Kolsi L, Kata S, Sahoo B (2017) A Review of Nano Fluid Role to Improve the Performance of the Heat Pipe Solar Collectors. Energy Procedia 109:417–24. https://doi.org/10.1016/j.egypro.2017.03.044

[5] Palanikumar G, Shanmugan S, Vengatesan C, Selvaraju P (2019) Evaluation of fuzzy inference in box type solar cooking food image of thermal effect. Environ Sustain Indic 1–2:100002. https://doi.org/10.1016/j.indic.2019.100002

[6] Bhavani S, Shanmugan S, Selvaraju P, Monisha C, Suganya V (2019) Fuzzy Interference

576 Treatment applied to Energy Control with effect of Box type Affordable Solar Cooker.
577 Mater Today Proc 18:1280–90. https://doi.org/10.1016/j.matpr.2019.06.590
578 [7] Palanikumar G, Shanmugan S, Chithambaram V (2021) Solar cooking thermal image
579 processing applied to time series analysis of fuzzy stage and inconsiderable Fourier
580 transform method. Mater Today Proc 34:460–8.
581 https://doi.org/10.1016/j.matpr.2020.02.664
582 [8] Venugopal D, Chandrasekaran J, Janarthanan B, Shanmugan S, Kumar S (2012) Parametric
583 optimization of a box-type solar cooker with an inbuilt paraboloid reflector using Cramer's
584 rule. Int J Sustain Energy 31:213–27. https://doi.org/10.1080/1478646X.2011.558197
585 [9] Thamizharasu P, Shanmugan S, Gorjian S, Pruncu CI, Essa FA, Panchal H, Mooli Harish
586 (2022) Improvement of Thermal Performance of a Solar Box Type Cooker Using SiO_2/TiO_2
587 Nanolayer. Silicon 14:557–565 https://doi.org/10.1007/s12633-020-00835-1
588 [10] Thamizharasu P, Shanmugan S, Sivakumar S, Pruncu CI, Kabeel AE, Nagaraj J, Lakshmi
589 SarvaniVidela, Vijai Anand K, Lambertig L, MeenaLaadh (2021) Revealing an OSELM
590 based on traversal tree for higher energy adaptive control using an efficient solar box
591 cooker. Sol Energy 2021;218:320–36. https://doi.org/10.1016/j.solener.2021.02.043
592 [11] Palanikumar G, Shanmugan S, Chithambaram V, Gorjian S, Pruncu CI, Essa FA, Kabeel
593 AE, HiteshPanchal, Janarthanan B,HosseinEbadil, Ammar H.Elsheikh, Selvaraju P (2021)
594 Thermal investigation of a solar box-type cooker with nanocomposite phase change
595 materials using flexible thermography. Renew Energy 178:260–82.
596 https://doi.org/10.1016/j.renene.2021.06.022
597 [12] Palanikumar G, Shanmugan S, Janarthanan B, Sangavi R, Geethanjali P (2019) Energy and
598 Environment control to Box type Solar Cooker and Nanoparticles mixed bar plate coating
599 with Effect of Thermal Image cooking pot. Mater Today Proc 18:1243–55.
600 https://doi.org/10.1016/j.matpr.2019.06.586
601 [13] Palanikumar G, Shanmugan S, Chithambaram V, Selvaraju P (2020) Synthesis,
602 characterization of Ta2O5 nanoparticles with doping SnO_2– Ag on solar absorber material
603 and designs analysis of energy production for solar cooker. Mater Today Proc 30:190–6.
604 https://doi.org/10.1016/j.matpr.2020.05.740
605 [14] Shinde YH, Gudekar AS, Chavan P V., Pandit AB, Joshi JB (2016) Design and development
606 of energy efficient continuous cooking system. J Food Eng 168:231–9.

https://doi.org/10.1016/j.jfoodeng.2015.07.042

[15] Sharafeldin MA, Gróf G (2018) Evacuated tube solar collector performance using CeO_2/water nanofluid. J Clean Prod 185:347–56. https://doi.org/10.1016/j.jclepro.2018.03.054

[16] Khallaf AM, Tawfik MA, El-Sebaii AA, Sagade AA (2020) Mathematical modeling and experimental validation of the thermal performance of a novel design solar cooker. Sol Energy 207:40–50. https://doi.org/10.1016/j.solener.2020.06.069

[17] Hosseinzadeh M, Sadeghirad R, Zamani H, Kianifar A, Mirzababaee SM (2021) The performance improvement of an indirect solar cooker using multi-walled carbon nanotube-oil nanofluid: An experimental study with thermodynamic analysis. Renew Energy 165:14–24. https://doi.org/10.1016/j.renene.2020.10.078

[18] Mallikarjuna K, Santhoshkumar Reddy Y, Hemachandra Reddy K, Sanjeeva Kumar PV (2021) A nanofluids and nanocoatings used for solar energy harvesting and heat transfer applications: A retrospective review analysis. Mater Today Proc 37:823–34. https://doi.org/10.1016/j.matpr.2020.05.833

[19] Liu B, Wang C, Bazri S, Badruddin IA, Orooji Y, Saeidi S, et al (2020) Optical properties and thermal stability evaluation of solar absorbers enhanced by nanostructured selective coating films. Powder Technol 377:939–57. https://doi.org/10.1016/j.powtec.2020.09.040

[20] Eidan AA, AlSahlani A, Ahmed AQ, Al-fahham M, Jalil JM (2018) Improving the performance of heat pipe-evacuated tube solar collector experimentally by using Al_2O_3 and CuO/acetone nanofluids. Sol Energy 173:780–8. https://doi.org/10.1016/j.solener.2018.08.013

[21] Vijayakumar P, Kumaresan G, Gokul Kumar S, Eswaran M (2020) A review on applications of nanofluid in evacuated tube heat pipe integrated with compound parabolic concentrator. Mater Today Proc 45:1227–32. https://doi.org/10.1016/j.matpr.2020.04.250

[22] Vengadesan E, Senthil R (2021) Experimental investigation of the thermal performance of a box type solar cooker using a finned cooking vessel. Renew Energy 171:431–46. https://doi.org/10.1016/j.renene.2021.02.130

[23] Hosseinzadeh M, Sadeghirad R, Zamani H, Kianifar A, Mirzababaee SM, Faezian A (2021) Experimental study of a nanofluid-based indirect solar cooker: Energy and exergy analyses. Sol Energy Mater Sol Cells 221:110879. https://doi.org/10.1016/j.solmat.2020.110879

[24] Shehayeb S, Deschanels X, Ghannam L, Karame I, Toquer G (2021) Tandem selective photothermal absorbers based on EPD of CuO colloidal suspension coupled with dip-coated silica. Surf Coatings Technol 408:126818. https://doi.org/10.1016/j.surfcoat.2020.126818

[25] Ghamsari MS, Alamdari S, Razzaghi D, Arshadi Pirlar M (2019) ZnO nanocrystals with narrow-band blue emission. J Lumin 205:508–18. https://doi.org/10.1016/j.jlumin.2018.09.064

[26] Alamdari S, Tafreshi MJ, Ghamsari MS (2019) Strong yellow-orange emission from aluminum and Indium co-doped ZnO nanostructures with potential for increasing the color gamut of displays. Appl Phys A 125:165. https://doi.org/10.1007/s00339-019-2451-x

[27] Alamdari S, Tafreshi MJ, Ghamsari MS (2017) The effects of indium precursors on the structural, optical and electrical properties of nanostructured thin ZnO films. Mater Lett 197:94–7. https://doi.org/10.1016/j.matlet.2017.03.113

[28] Alamdari S, Ghamsari MS, Ara MHM, Efafi B (2015) Highly concentrated IZO colloidal nanocrystals with blue/orange/red three-colors emission. Mater Lett 158:202–4. https://doi.org/10.1016/j.matlet.2015.06.001

[29] Vafaee M, Sasani Ghamsari M, Radiman S (2011) Highly concentrated zinc oxide nanocrystals sol with strong blueemission. J Lumin 131:155–8. https://doi.org/10.1016/j.jlumin.2010.09.042

[30] Said Z, Hachicha AA, Aberoumand S, Yousef BAA, Sayed ET, Bellos E (2021) Recent advances on nanofluids for low to medium temperature solar collectors: energy, exergy, economic analysis and environmental impact. Prog Energy Combust Sci 84:100898. https://doi.org/10.1016/j.pecs.2020.100898

[31] Abd-Elhady MS, Abd-Elkerim ANA, Ahmed SA, Halim MA, Abu-Oqual A (2020) Study the thermal performance of solar cookers by using metallic wires and nanographene. Renew Energy 153:108–16. https://doi.org/10.1016/j.renene.2019.09.037

[32] Arulraj Simon Prabu, Venkatesan Chithambaram, Maria Anto Bennet, Sengottaiyan Shanmugan, Catalin Iulian Pruncu, Luciano Lamberti, Ammar Hamed Elsheikh, Hitesh Panchal & Balasundaram Janarthanan (2022) Microcontroller PIC 16F877A standard based on solar cooker using PV—evacuated tubes with an extension of heat integrated energy system. Environmental Science and Pollution Research 29:15863–15875. https://doi.org/10.1007/s11356-021-16863-2

Figures

Figure 1

(a) Photos of preparing leaf extract from Acalypha Indica leaves.

(b). The prepared ZnO/Acalypha Indica leaf extract.

(c). The prepared ZnO/Acalypha Indica stem extract.

(d). ZAE chemical bond energy absorption process.

Figure 2

(a). XRD analysis of ZnO/Acalypha Indica extract.

(b). FTIR analysis of ZAE.

(c). The UV analysis ZAE.

(d) SEM analysis of ZAE.

(e) EDAX analysis of ZAE.

Figure 3

(a) An experimental setup of the solar cooker that coated with ZAE and fixed in a cooking vessel with an ETC, a battery charge controller.

(b) The ZAE coated in Nichrome heating coil and different food cooked by the solar cooker.

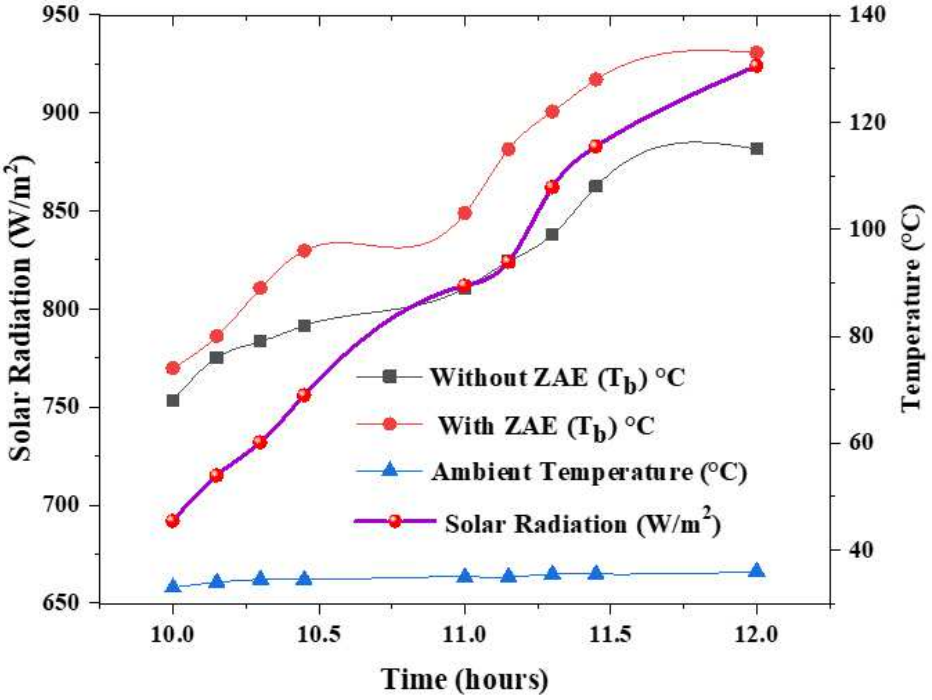

A

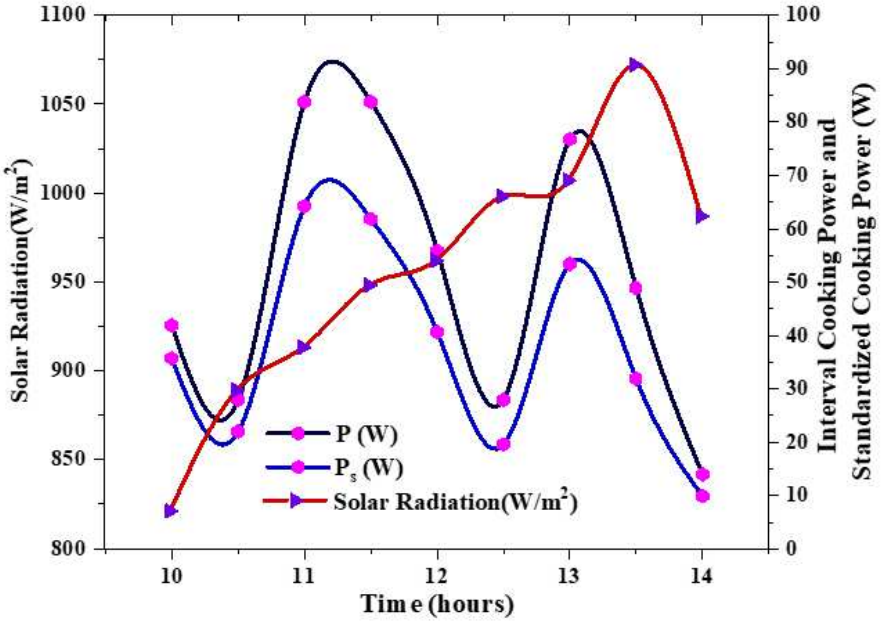

B

Figure 4

(a) Variation of solar radiation and temperature of the cooking vessel (T_b) with and without ZAE.

(b) shows a variety of interval and Standardized cooking power.

Figure 5

(a) Variation of solar radiation and ambient temperature in the solar cooker average values from June 2020 to June 2021.

(b) shows a variation of the side, base, and lid of the cooking vessel with and without a coating of ZAE in one-micron levels.

(c) shows various theoretical and experimental values of the temperature of the side, base, and lid of the cooking vessel.

(d) shows a variation of the cooking fluid’s temperature.

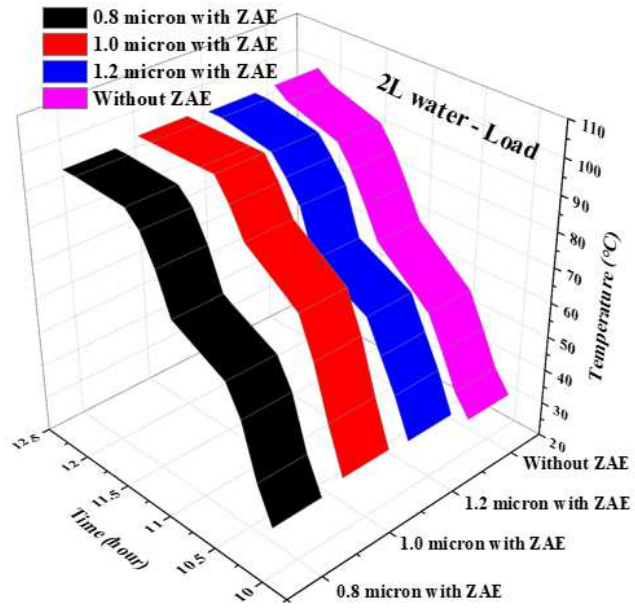

A

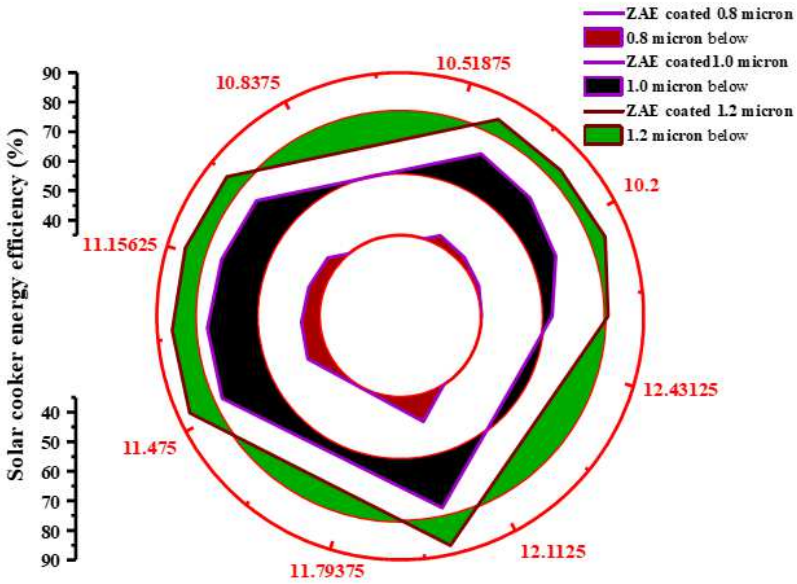

B

Figure 6

(a) The water temperature in the cooking pot for different coated ZAE micron levels. (b) Average energy efficiency of the solar cooker for different thicknesses of ZAE coating.